

Sensitivity of Earthquakes to Atmospheric Anomalies Triggered over South-Western Region of South Asia

Ahmad, B.^{1, 2}, A. Hassan³, N. Mahmood²

Abstract

Earthquakes brings great destruction to the natural environment including landscapes, rivers, wild life, people and infrastructure. This is a natural disaster, hence, cannot be controlled. However to save human lives and property, this natural calamity can be avoided by predicting its location of occurrence and sensitivity to natural anomalies ahead of time. In the past various factors with possible linkages were studied to predict this phenomenon. In this research, atmospheric anomalies are investigated for their possible potential to stimulate earthquakes. Based on analyzed observations it is hypothesized that prior seismicity of an area usually triggers rainfall before an earthquake. The relationship of rainfall and other atmospheric variables with the earthquake were determined using the sensitivity analysis. This analysis graphically showed that in most cases rainfall occurs before an earthquake. Moreover, by depending on the positive results of sensitivity analysis, factor analysis was conducted. This brought forward results which gave statistical relationships of different atmospheric variables with high magnitude and shallow depth earthquakes in the South-Western region of South Asia.

Introduction

Research works on factors triggering earthquake are numerous. Most are just assumptions which are supported by forced facts, while some assumptions are supported by natural events, evidences and results. However, both assumptions and evidences are accepted and may be considered for further investigation. There are various earthquake precursors including a synchronous emission spectra of a low frequency electromagnetic radiation by rocks under stress due to plate-tectonic forces (Varotsos et al. 2017), electric and magnetic field (Larkina et al. 1989), concentration changes of gas emissions specially of Radon prior to occurrence of nearby earthquakes (Lomnitz 1996), groundwater level changes (Martinelli 2000), ground temperature changes (Lachenbruch and Sass 1992), surface deformations (Rikitake 1968), and prior seismicity (Reasenberg 1999). These precursors have been reliable and were researched countless times. In many case events, they accurately predicted the earthquake however, in equally numerous instances no precursory phenomena of significance were observed, which is compelling us to understand that, aside from the main most reliable precursors there must be some significant phenomenon which has been ignored.

During the occurrence of earthquakes, potential energy (strain energy and gravitational energy) stored in earth is released through seismic waves. The two main types of seismic waves are body waves and surface waves. The body waves include P waves and S waves, while the surface waves include Love waves and Rayleigh waves. While P waves reach the surface layer before destruction occurs, major devastation is caused by the surface waves. (Kanamori 2001).

The atmospheric variables like rainfall capable of being a precursor to the earthquakes was vastly ignored, as per logic it was believed that a weather phenomenon was unlikely to trigger an incoming earthquake phenomenon. Nevertheless in recent works, seismicity is shown to stimulate certain atmospheric anomalies resulting in different atmospheric phenomenon like increased values of surface-latent heat flux (SLHF) (Zhang et al. 2013) and prior rainfall events of (3-23days) before an earthquake in vicinity (Mansouri Daneshvar et al. 2014). Latent heat release due to air ionization (Pulinets et al. 2006), emanation of warm gases and local greenhouse effect (Tronin et al. 2002; Tramutoli et al. 2005), and stress-induced thermal effects due to friction and fluids (Wu and Liu 2009) can be explained as possible precursors. The air above the fault prior to the earthquake is ionized due to build up stress in igneous rocks (Freund et al. 2006).

¹ burhanahmadkhan@gmail.com

² Pakistan Meteorological Department, Pitrus Bukhari Road, Sector H-8/2, Islamabad, Pakistan.

³Department of Earth and Environmental Sciences, Bahria University, Islamabad, Pakistan.

During subordinate rainfall, the condensation of water vapors ions are in the center (Svensmark et al. 2007). Latent heat of evaporation is released during the transition phase of water vapors ions during condensation (Pulinets and Ouzounov 2011). The Radon near active faults ionizes these molecules of atmospheric gases. The following heat release is believed to be an earthquake precursory (Pulinets et al. 2015). Hence many previous researches point towards seismicity induced rainfall preceding various earthquake events. It was indicated that almost half of the total magnitude 3.5 earthquakes had strain responses after a rainfall event (Yamauchi 1987).

There are many similar studies related to ours, focusing in proving a weak assumption. We choose to find evidence for an atmospheric phenomenon as an earthquake precursor in seismological region including a large part of northwestern Pakistan and small parts of Afghanistan and Tajikistan. Our assumption is that pre-seismic activity before the main shock will induce certain atmospheric phenomena like abnormal increase in SLHF and rainfall (hence increased melting of snow and decrease in snow depth). Instead of getting a forced analysis for the benefit of proving our assumption, this research focuses on getting natural analysis from the general data.

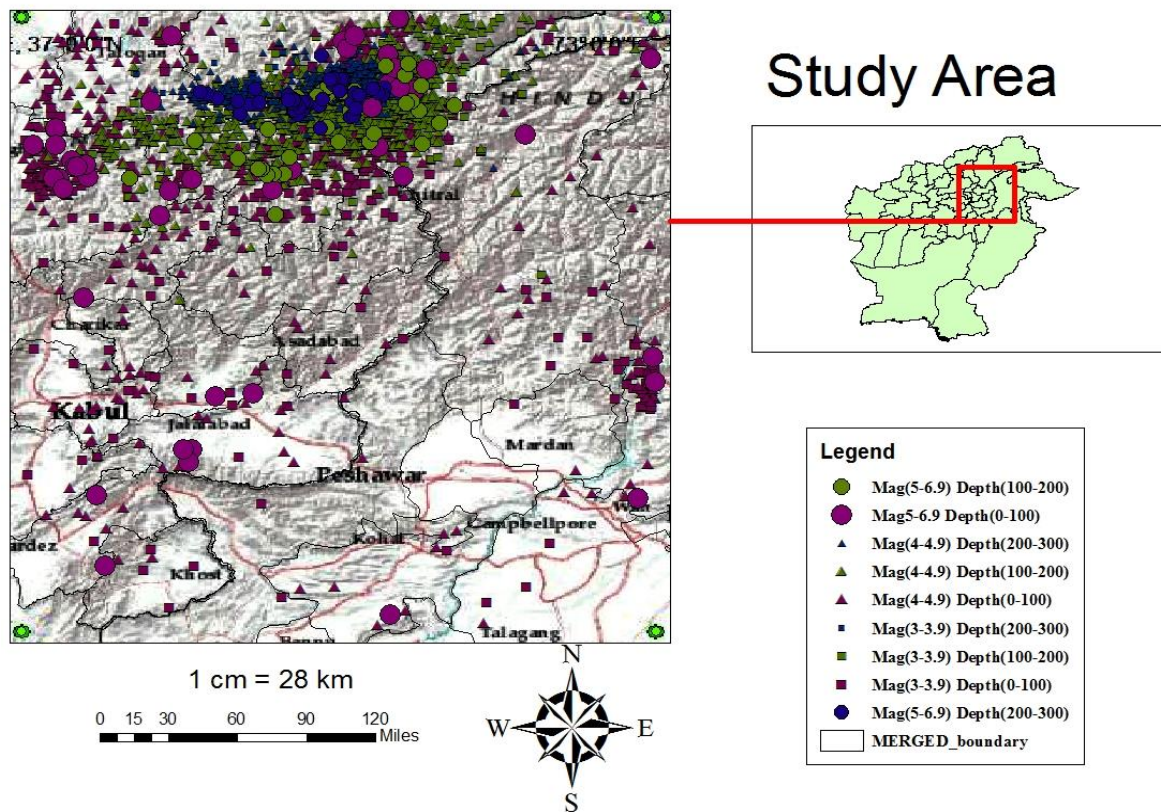


Figure 1: Study area for the research. The top left area of the study area is Hindukush Fault region, where the maximum concentration of earthquake activity is shown. The rest of the map shows very less earthquake activity as compared to the north-western area beyond Pakistan's boundary in Afghanistan.

Acquisition of Data

The earthquake data was obtained from Pakistan Meteorological Department (PMD). The data consisted of date, time, coordinates, epi-centers and magnitude. The date ranged from 01 Jan 2000 to 12 Mar 2016. Multiple earthquake events during a single day were included in the analysis. This data was used to map earthquake density with bifurcation of magnitude and depth classification preset in the study area (Figure 1).

Now to make sense of the data we included the dates where earthquake event did not occur. Moreover, to avoid the duplication of dates where multiple earthquakes occurred on the same day, the earthquakes data of the same day were combined. Using the date as the primary key, the depth and the magnitude of earthquakes were averaged. This earthquake data was utilized and compiled into several tables and graphs for better understanding of the data.

Table 1: Yearly frequency of the earthquakes as per depth.

Depth	Shallow (0-80km)	Intermediate (81-300km)	Deep(above300km)	Blank
Duration	No. of Earthquakes	No of Earthquakes	No of Earthquakes	Total number of Earthquakes
2000	27	111	1	139
2001	26	153	0	179
2002	99	140	0	239
2003	44	82	0	126
2004	46	122	0	168
2005	122	150	0	272
2006	78	155	0	233
2007	28	242	0	270
2008	40	280	0	320
2009	9	46	0	55
2010	13	55	0	68
2011	31	52	0	83
2012	18	85	0	103
2013	11	130	0	141
2014	19	118	0	137
2015	12	190	1	203
Total	623	2111	2	2736

In a preliminary analysis, earthquakes frequency in shallow depth is shown where the frequency increases from 2000-2005 and then decreases from 2005 onwards (Table 1). In intermediate depth preset, the frequency is shown to increase from 2000-2008 and then is shown to decrease to extremely low in 2009 then starts increasing from 2010 onwards. The frequency of earthquakes in an intermediate depth is greater than earthquakes of shallow depth. The total yearly frequency of earthquakes also increases from 2000-2008, then again increases from extremely low frequency to high frequency from 2009 onwards.

In further data diagnosis, we found sensitivity of earthquakes to their magnitude and depth (Table 2). The greatest frequency of earthquakes had magnitudes from (4-4.9) with an intermediate depth of 81-300 km. Moreover, we observed, that there was almost no earthquake of mag 3-3.9 with shallow and intermediate depths from the year 2009-2015. However numerous earthquakes occurred in the years 2000-2008. In all the sections one common aspect was found that from 2000-2008 the frequency of earthquakes increased followed by an abrupt halt of earthquakes occurrence in 2009 with gradual increase in the frequency of the earthquakes thereafter.

In pursuance of acquisition of atmospheric data we accessed European Centre for Medium-Range Weather Forecasts (ECMWF) ERA Interim daily products. The ERA Interim provides long-term historical datasets available readily for research (Dee et al., 2011).

A total of five parameters were acquired, namely total precipitation, 2 m temperature, snow melt, snow depth and SLHF. The time interval was set to be from 01 Jan, 2000 to 31 Dec, 2015. The time for measuring data was 12Z with a 12 hour cycle. The type of measuring level was near the surface. The area was custom set within the coordinates 69E 73W 33S 37N. The spatial grid resolution was selected to be 0.125m × 0.125m for fine scale assessment.

Table 2: For each set range of Magnitude, the number of Earthquakes with shallow and intermediate depth categorized on yearly basis.

Years	3-3.9 (Magnitude)		4-4.9		5-5.9		Total Frequency
	Shallow (AF) 0-80 km	Intermed. 81-300km	Shallow(AF) 0-80 km	Intermed. 81-300 km	Shallow(AF) 0-80 km	Intermed. 81-300 km	
2000	9	36	17	71	1	2	136
2001	9	57	15	93	2	1	177
2002	36	61	57	72	5	4	235
2003	12	26	31	54	1	2	126
2004	19	30	24	86	3	4	166
2005	66	54	52	90	4	5	271
2006	46	54	32	100	0	1	233
2007	6	42	21	192	1	7	269
2008	16	81	21	188	1	11	318
2009	1	0	5	38	3	5	52
2010	0	0	10	46	3	8	67
2011	0	0	31	45	0	7	83
2012	0	0	14	80	4	5	103
2013	0	1	10	123	1	6	141
2014	1	0	17	112	1	6	137
2015	0	1	12	182	0	5	200
Total	221	443	369	1572	30	79	2714

Sensitivity Analysis

Initially the earthquake and ERA Interim datasets are analyzed using ncBrowse (https://www.nodc.noaa.gov/woce/woce_v3/wocedata_1/utills/netcdf/ncbrowse/index.htm). Total precipitation prior to earthquake events are analyzed. In this analysis, a month time interval is selected on basis of 10 most dangerous earthquakes of highest magnitude and shallowest depth. A period of 15 days prior and after the earthquake is observed based on exact coordinates of depth, with fixed latitude and varying longitudes (69E-73W), as well as with fixed longitude and varying latitudes (33S-37N). Various results were obtained (Figures 2-7).

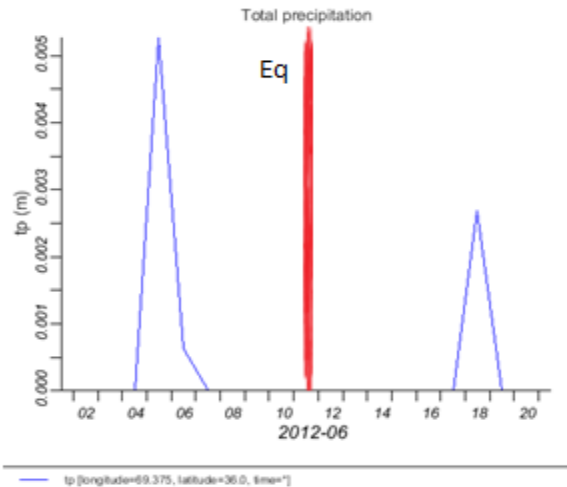


Figure 2: Total precipitation at the exact coordinates of earthquake epicenter with a time interval of 10 days prior and after the earthquake occurrence. The horizontal axis shows the dates while vertical axis shows total precipitation in meters. The figure shows a 5mm before and a 2.8mm rainfall after the earthquake of 11 Jun, 2012.

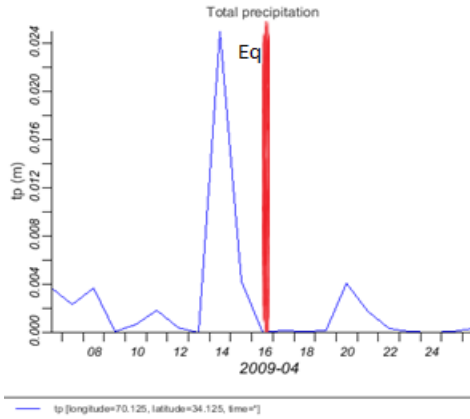


Figure 3: Total precipitation at the exact coordinates of earthquake epicenter with a time interval of 10 days prior and after the earthquake occurrence. The horizontal axis shows the dates while vertical axis shows total precipitation in meters. The figure shows a 24 mm before and a 4mm rainfall after the earthquake at 16 Apr, 2009.

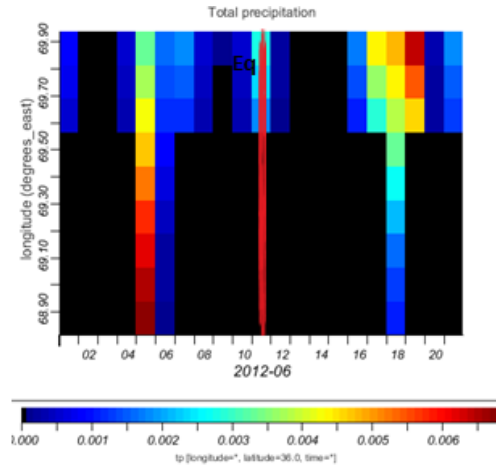


Figure 4: Total precipitation at the exact latitude and variable longitude from the earthquake epicenter with a time interval of 10 days prior and after the earthquake occurrence. The horizontal axis shows the dates while vertical axis shows total precipitation in meters. The figure shows rainfall varying from 0 mm to 7mm before and zero mm to 5mm after the earthquake on 11 Jun,2012.

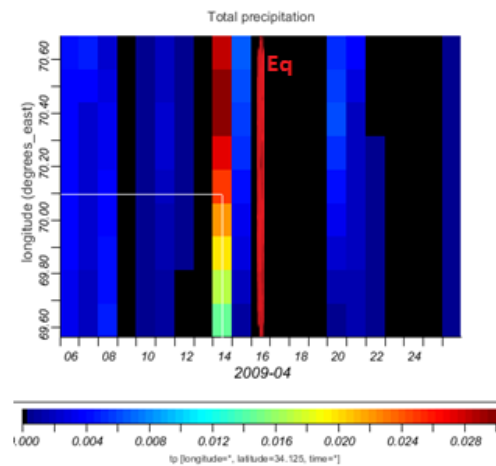


Figure 5: Total precipitation at the exact latitude and variable longitude from the earthquake epicenter with a time interval of 10 days prior and after the earthquake occurrence. The horizontal axis shows the dates while vertical axis shows total precipitation in meters. The figure shows rainfall varying from 12mm to 28mm before and 0 mm to 5mm after the earthquake on 16 Apr, 2009.

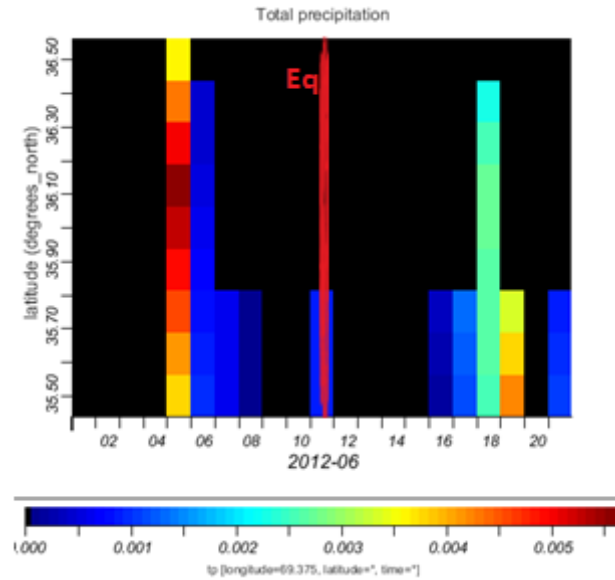


Figure 6: Total precipitation at the exact longitude and variable latitude from the earthquake epicenter with a time interval of 10 days prior and after the earthquake occurrence. The horizontal axis shows the dates while vertical axis shows total precipitation in meters. The figure shows rainfall varying from 3.5mm to 6mm before and a 2.5mm after the earthquake on 11 Jun, 2012.

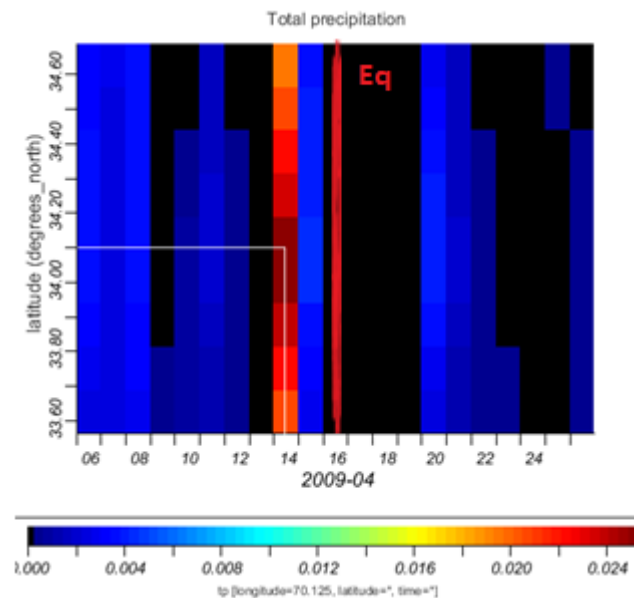


Figure 7: Total precipitation at the exact longitude and variable latitude from the earthquake epicenter with a time interval of 10 days prior and after the earthquake occurrence. The horizontal axis shows the dates while vertical axis shows total precipitation in meters. The figure shows rainfall varying from 20 mm to 25 mm before and 4mm after the earthquake on 16 Apr, 2009.

The sensitivity analysis was performed to gain general idea to build a hypothesis and to confirm if our primary assumption can be applied. So, this was viewed as a primary test for further analysis.

To further our testing of the atmospheric precursors, we made sensible understanding of the data containing the precursors (total precipitation, 2m temperature, snow melt, snow depth and SLHF). The data contained daily value of these precursors on the coordinates 69E 73W 33S 37N. Our preliminary objective was to find a link between earthquake and these atmospheric variables. As per past research, there usually is a

linkage of precursors with actual predicted earthquake events, hence the first step was to find the necessary natural evidences to support our assumption.

The atmospheric variables in the data were averaged over the whole area of coordinates 69E 73W 33S 37N on daily basis with a time frame starting from 01 Jan, 2000 to 31 Dec, 2015. For convenience of understanding, the unit of total precipitation was changed from m to mm and the unit for SLHF was changed from J/M^2 to W/m^2 . While the rest of the atmospheric parameter's unit remained unchanged throughout the research. The earthquake data was synchronized with the atmospheric variables data as per dates. Then filters were applied to both magnitude and epicenter of the earthquakes. The magnitude was set to be greater and equal to 5 and epicenter was set to less and equal to 80 meters. The filtered results showed 26 main earthquakes (Table 3), which were used for sensitivity analysis. In the sensitivity analysis, several parameters are plotted together to observe the sensitivity of each atmospheric variable over the other and on earthquakes. Each earthquake date was set to be between 15 days for any type of variability to be made visible. More earthquakes occurrences were added to be analyzed later aside from this main data.

Table 3: The geographical characteristics of 26 major earthquakes in the Northern Pakistan, including date, magnitude, hypocenter depth, epicenter latitude, epicenter longitude

No.	Date	Magnitude	Depth (km)	latitude (°)	longitude (°)
1	02/01/2001	5.3	33.00	36.1670	69.0730
2	01/06/2001	5.0	62.10	35.1690	69.3890
3	25/03/2002	6.1	8.00	36.0620	69.3150
4	27/03/2002	5.6	10.00	36.0230	69.3380
5	12/04/2002	5.9	10.00	35.9590	69.4170
6	25/04/2003	5.1	66.90	36.6600	71.5550
7	15/07/2004	5.4	47.50	35.8750	70.5790
8	18/07/2004	5.2	10.00	33.4260	69.5240
9	16/10/2004	5.0	65.10	36.7930	71.0540
10	01/07/2005	5.6	63.10	36.5690	71.3200
11	31/08/2005	5.0	17.60	36.2690	69.2140
12	08/10/2005	5.2	10.00	34.6210	72.9960
13	18/10/2005	5.0	10.00	34.7860	72.9850
14	11/02/2007	5.1	53.80	36.7280	72.9710
15	05/10/2008	6.0	10.00	33.8860	69.4700
16	21/12/2008	5.0	74.40	35.9620	71.4070
17	16/04/2009	5.2	5.90	34.1850	70.0760
18	30/10/2009	5.1	30.40	34.1810	70.0200
19	06/05/2010	5.0	50.60	33.1080	71.3280
20	10/10/2010	5.2	33.20	33.8690	72.8870
21	15/11/2010	5.2	34.10	34.5490	70.4580
22	11/06/2012	5.7	16.00	36.0230	69.3510
23	25/09/2012	5.2	30.30	36.2770	69.2110
24	14/10/2012	5.1	50.20	36.1670	69.2160
25	24/04/2013	5.5	63.80	34.5260	70.2200
26	27/09/2014	5.0	29.16	36.4517	69.8145

The results showed that only 5 of the major earthquakes occurrences did not display any significant atmospheric precursors before the earthquake, nevertheless more than 21 occurrences of major earthquake displayed some atmospheric precursors (see e.g. Figures 8-11) which were beneficial for further analysis.

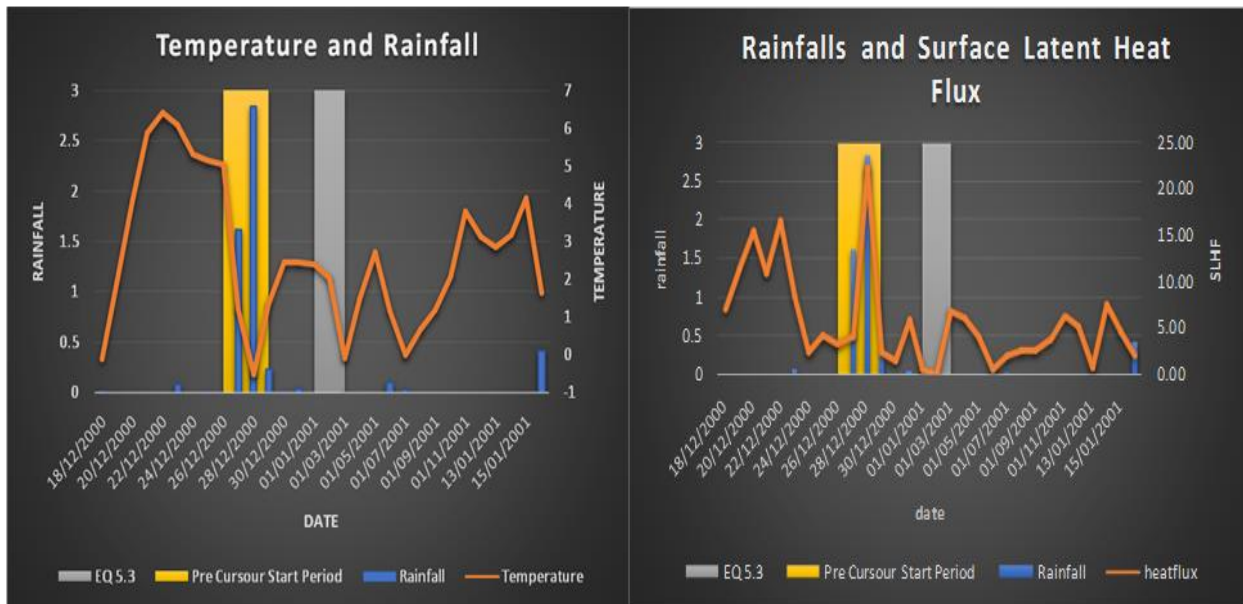


Figure 8: The graph shows the sensitivity analysis of both (rainfall, temperature and earthquake occurrence) and (rainfall, SLHF and earthquake occurrence), where in both the graphs show a rainfall of 2.8mm occurred four days prior to earthquake. The temperature falls dramatically during the rainfall event and rises dramatically till the earthquake event. The SLHF abruptly rises during the rainfall event then falls till the earthquake event.

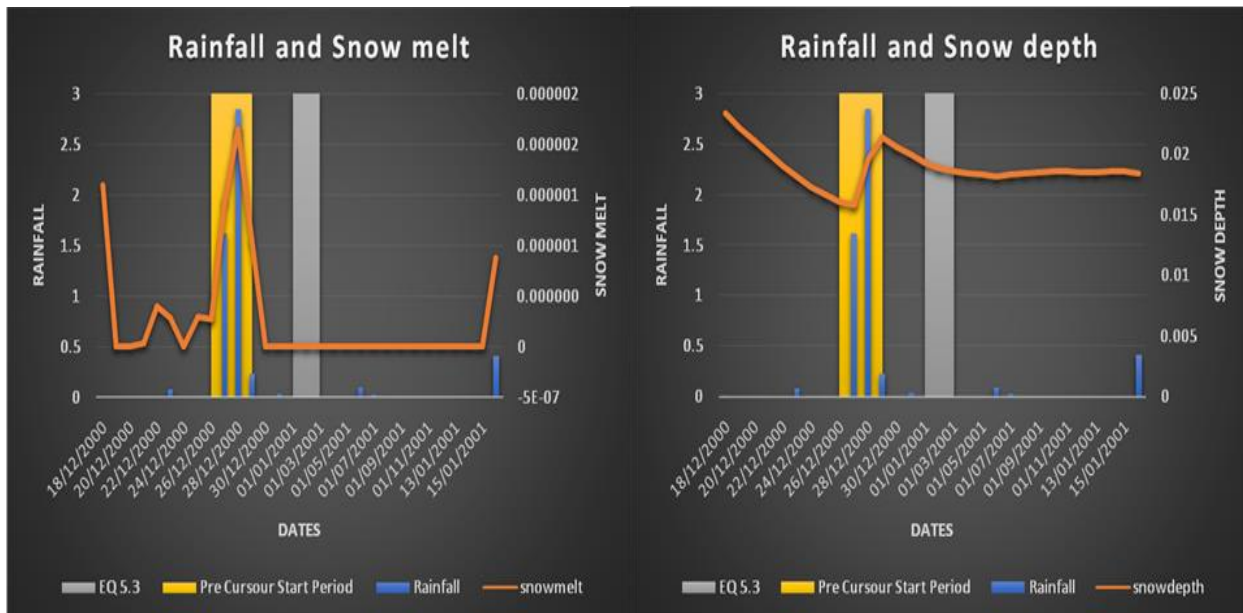


Figure 9: The graph shows sensitivity analysis of both (rainfall, snow melt and earthquake occurrence) and (rainfall, snow depth and earthquake occurrence), where both the graphs show a rainfall occurrence of 2.8mm four days prior to the earthquake. Rate of snow melt increases dramatically and snow depth rises abruptly during the precipitation event and falls till the earthquake event.

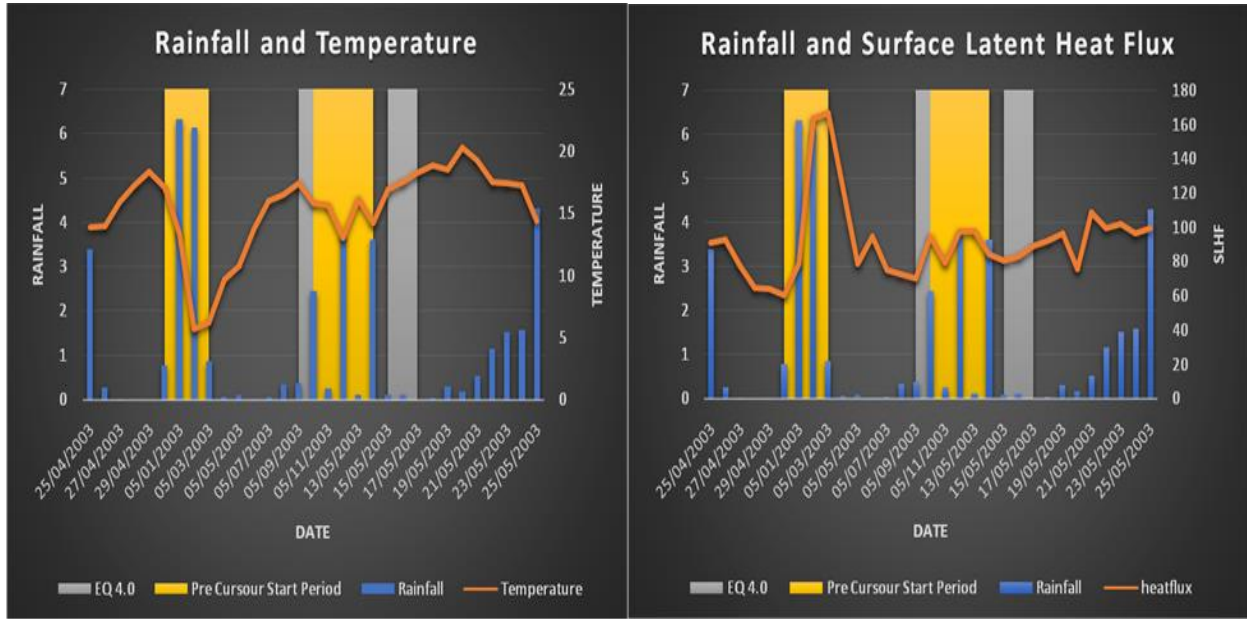


Figure 10: The graph shows sensitivity analysis of both (rainfall, temperature and earthquake occurrence) and (rainfall, SLHF and earthquake occurrence), where both the graphs show a rainfall occurrence of 6.2mm seven days prior to earthquake. The temperature falls dramatically during the rainfall event and rises dramatically till the earthquake event, whereas the SLHF rises abruptly during the rainfall event and then falls till the earthquake event.

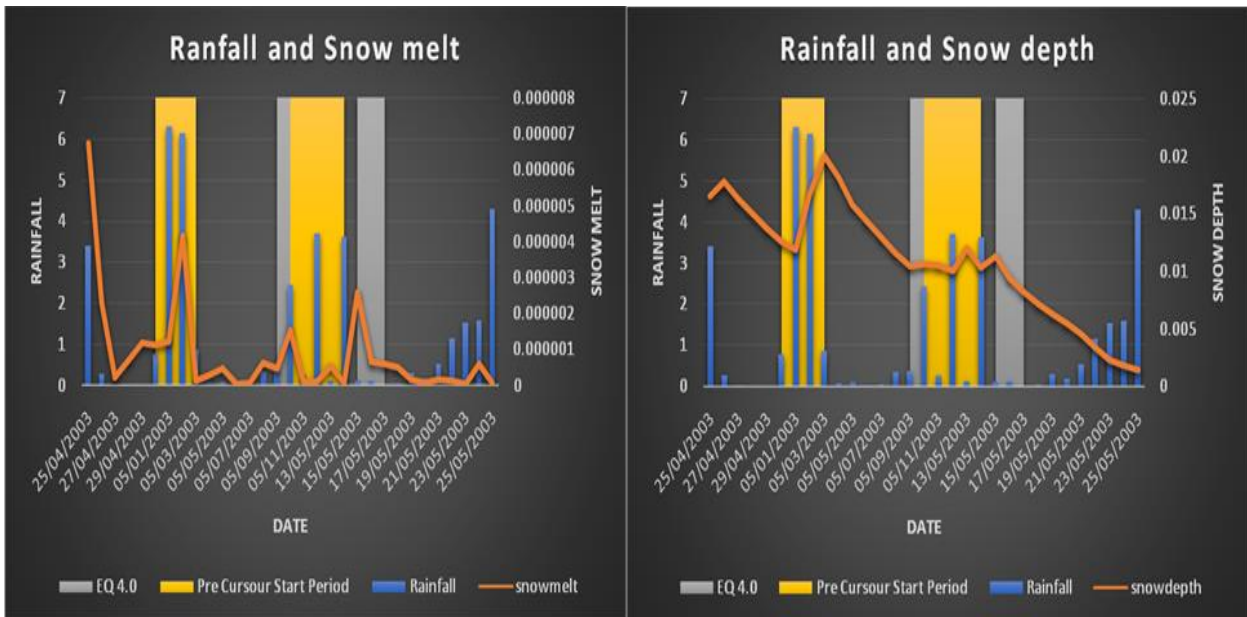


Figure 11: The graph shows sensitivity analysis of both (rainfall, snow melt and earthquake occurrence) and (rainfall, snow depth and earthquake occurrence), where both the graphs show a rainfall of 6.2mm occurred seven days prior to earthquake. The rate of snow melt increases dramatically and the snow depth rises abruptly during the precipitation event and falls till the earthquake event.

The Figures (8-11) present some of the strongest evidences supporting the assumption of atmospheric variables as a precursor before the main earthquake event. However, there exist evidences which do not support the assumption - fortunately they are few. Furthermore, there are also evidences where one or two atmospheric variables e.g. snow melt or snow depth not supporting the assumptions but other variables like

temperature, rainfall and SLHF supporting the assumption. In any case majority of main earthquake during sensitivity analysis, favor the acceptance of the assumption.

To further our sensitivity analysis, it was decided to filter the data using second standard deviation as a threshold. Hence the data was filtered as per rainfall greater than 5.13mm, temperature less than 17°C and snow melt greater than 6.10535E-05 m of water equivalent (Table 4). From the filtered data, 10 rainfall events were used for the atmospheric variable sensitivity analysis (an instance of the 10 events can be seen in Figures 12 and 13).

Table 4: Shows the days where rainfall > 5.13mm, temperature < 17°C and snow melt > 6.10535E-05 m of water equivalent occurred on the same day.

Count	Date	temperature	rainfall	Snow melt	Snow depth	SLHF
1	17/12/2000	0.25	7.84	0.00006	0.020	8.74
2	03/01/2002	2.27	5.71	0.00006	0.033	6.03
3	22/04/2004	11.06	5.98	0.00006	0.005	68.70
4	17/03/2005	8.73	7.39	0.00017	0.093	0.54
5	21/03/2005	5.41	5.84	0.00031	0.106	16.75
6	04/05/2005	11.09	10.18	0.00016	0.079	29.16
7	04/09/2006	5.46	13.04	0.00015	0.044	51.58
8	02/09/2007	1.54	5.72	0.00008	0.014	1.43
9	03/09/2007	0.82	8.58	0.00006	0.021	25.08
10	18/03/2007	7.79	6.12	0.00007	0.024	13.53
11	20/03/2007	6.13	5.40	0.00013	0.037	1.46
12	30/03/2007	11.85	5.40	0.00038	0.031	1.31
13	31/03/2007	9.73	18.38	0.00036	0.036	9.59
14	04/01/2007	7.23	11.63	0.00011	0.052	33.66
15	25/05/2008	13.59	8.91	0.00008	0.001	155.24
16	20/12/2008	-0.04	6.84	0.00007	0.015	1.57
17	16/01/2009	0.62	6.78	0.00007	0.026	8.83
18	03/03/2009	4.32	19.79	0.00012	0.044	26.80
19	05/04/2009	10.08	7.63	0.00026	0.066	49.87
20	17/05/2010	14.40	12.26	0.00013	0.051	99.99
21	20/02/2012	-0.16	8.37	0.00006	0.097	6.89
22	02/02/2013	0.96	6.20	0.00008	0.042	12.69
23	27/02/2013	-1.68	11.11	0.00007	0.089	86.63
24	03/09/2013	4.14	8.98	0.00009	0.085	7.23
25	13/03/2013	3.63	8.13	0.00009	0.089	0.24
26	02/03/2014	-1.64	5.37	0.00007	0.050	7.58
27	17/03/2014	5.40	21.63	0.00019	0.118	5.40
28	04/02/2014	5.18	10.55	0.00019	0.126	32.31
29	04/06/2014	5.96	9.74	0.00022	0.135	14.24
30	16/02/2015	4.79	7.38	0.00006	0.038	24.69
31	24/02/2015	1.99	26.05	0.00017	0.047	29.26
32	28/03/2015	8.27	12.87	0.00006	0.021	29.43

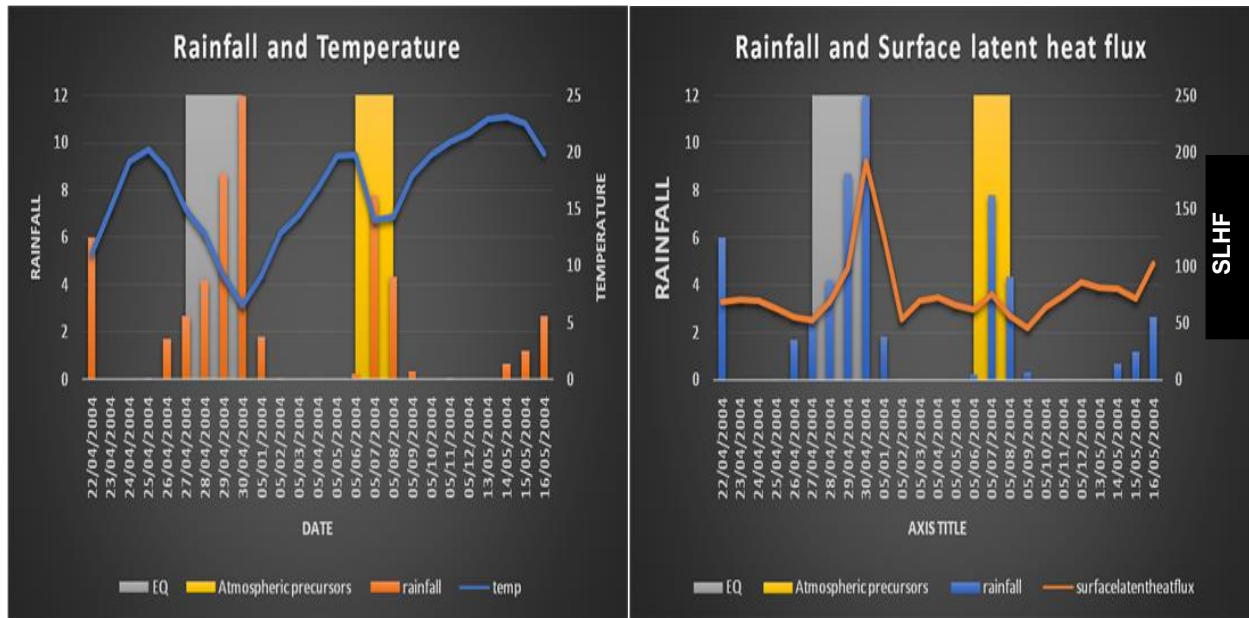


Figure 12: The graph shows the sensitivity analysis of both (rainfall, temperature and earthquake occurrence) and (rainfall, SLHF and earthquake occurrence), where both the graphs show a rainfall occurrence of 11.99mm six days prior to earthquake. The temperature falls dramatically during the rainfall event and rises dramatically till the earthquake event, whereas the SLHF rises abruptly during the rainfall event and then falls till the earthquake event.

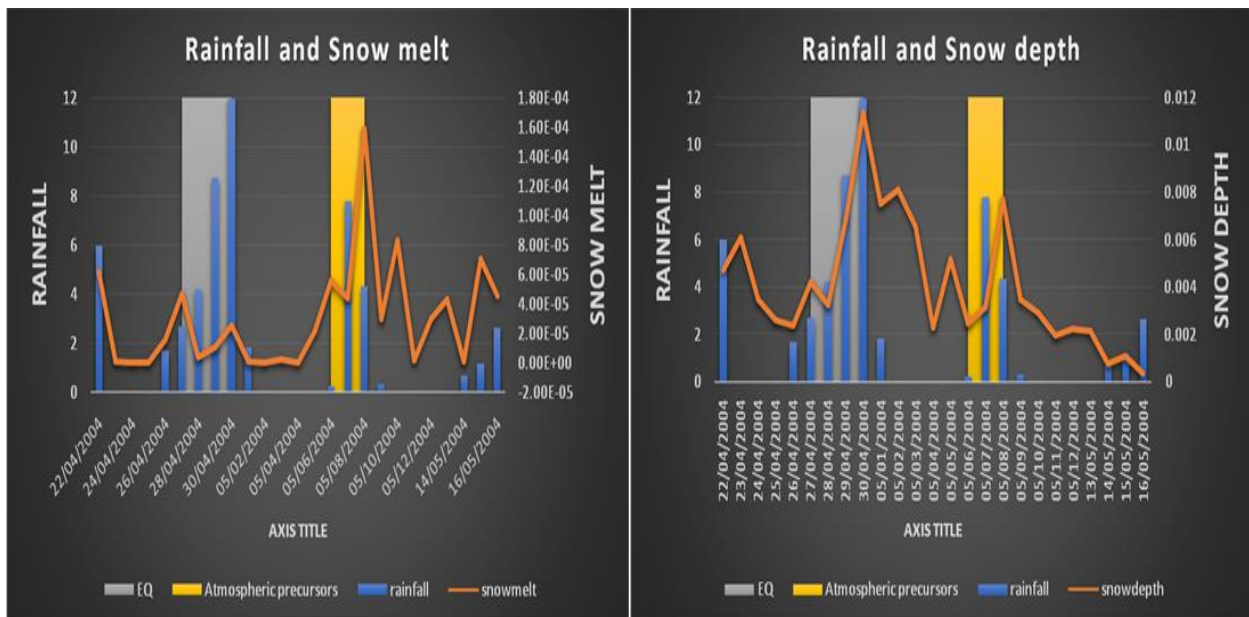


Figure 13: The graph shows sensitivity analysis of both (rainfall, snow melt and earthquake occurrence) and (rainfall, snow depth and earthquake occurrence), where both the graphs show a rainfall occurrence of 11.99mm six days prior to earthquake. In this case the rate of snow melt increases very lightly and snow depth rises abruptly during the rainfall event and falls till the earthquake event.

The major earthquakes chosen for further analysis were filtered as per second standard deviation of both magnitude (greater than 4) and depth (less than 152m). Before filtering the data, the total number of earthquakes occurred in 15 years were 2043, after filtering the data the number of earthquakes reduced to 875. Using these filtered data, the number of preceding days between major rainfall and earthquake event were calculated ranging from 3-23 days. Moreover, the accumulated rainfall and SLHF during the rainfall

were measured and likewise 522 earthquake events had major rainfall event before the earthquake, thus showing that 59.65% of major earthquake events had atmospheric variables as earthquake precursors. In 115 instances, the earthquakes were followed by accumulated rainfall of greater than 20 mm and in other 330 instances, the earthquakes were followed by accumulated rainfall of greater than 10 mm over the region. Furthermore, during 179 earthquake events the value of SLHF was greater than 82 Watts/m².

Preliminary Tests

Before moving to factor analysis, preliminary tests are performed to ensure that there is no violation of the assumption of normality, linearity and multi collinearity.

Multicollinearity Error Test

For multicollinearity error test, we take tolerance cutoff at 0.2, meaning tolerance less than 0.2 is worrisome or variance inflation factor greater than 5 can be problematic. By performing the multicollinearity test we got result with no multicollinearity between the independent variables (Table 5).

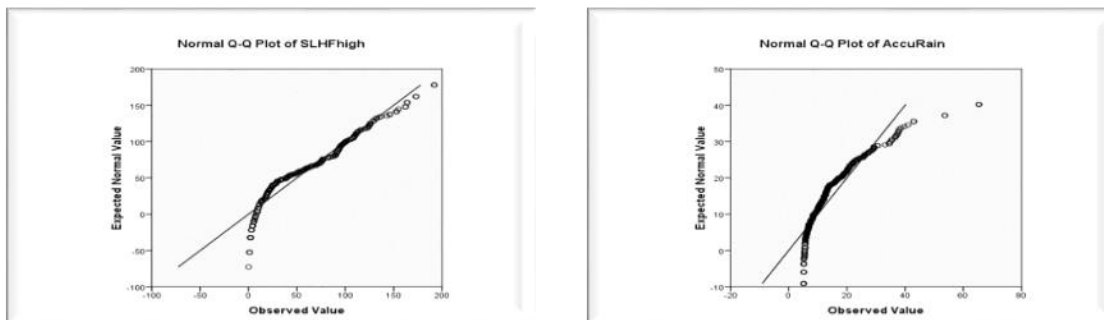
Table 5: Checking collinearity of independent variables between each other. Snow melt was taken as the dependent variable because it showed the maximum amount of variance inflation factor in the multicollinearity error test i.e. 3.519, which is still less than of 5.

Model		Collinearity Statistics	
		Tolerance	VIF
1	Mag	.981	1.019
	Depth	.965	1.036
	Sdepth	.724	1.381
	Pdays	.974	1.027
	Rain	.920	1.087
	Temp	.284	3.519
	SLHFhigh	.407	2.458
	AccuRain	.871	1.148
	SLHF	.334	2.990

Dependent Variable: Smelt

Normal q-q Plot Test

The q-q plot tells us whether the set of observations (data) are normally distributed. It also shows the linearity of the data. The assumption is that, if the set of data is normally distributed than a normal quantile-quantile (QQ) plot will result in an approximately straight line. This test is necessary to investigate the above assumption because, the following statistical inferencing procedures will assume that the data being analyzed is normally distributed (Figure 14).



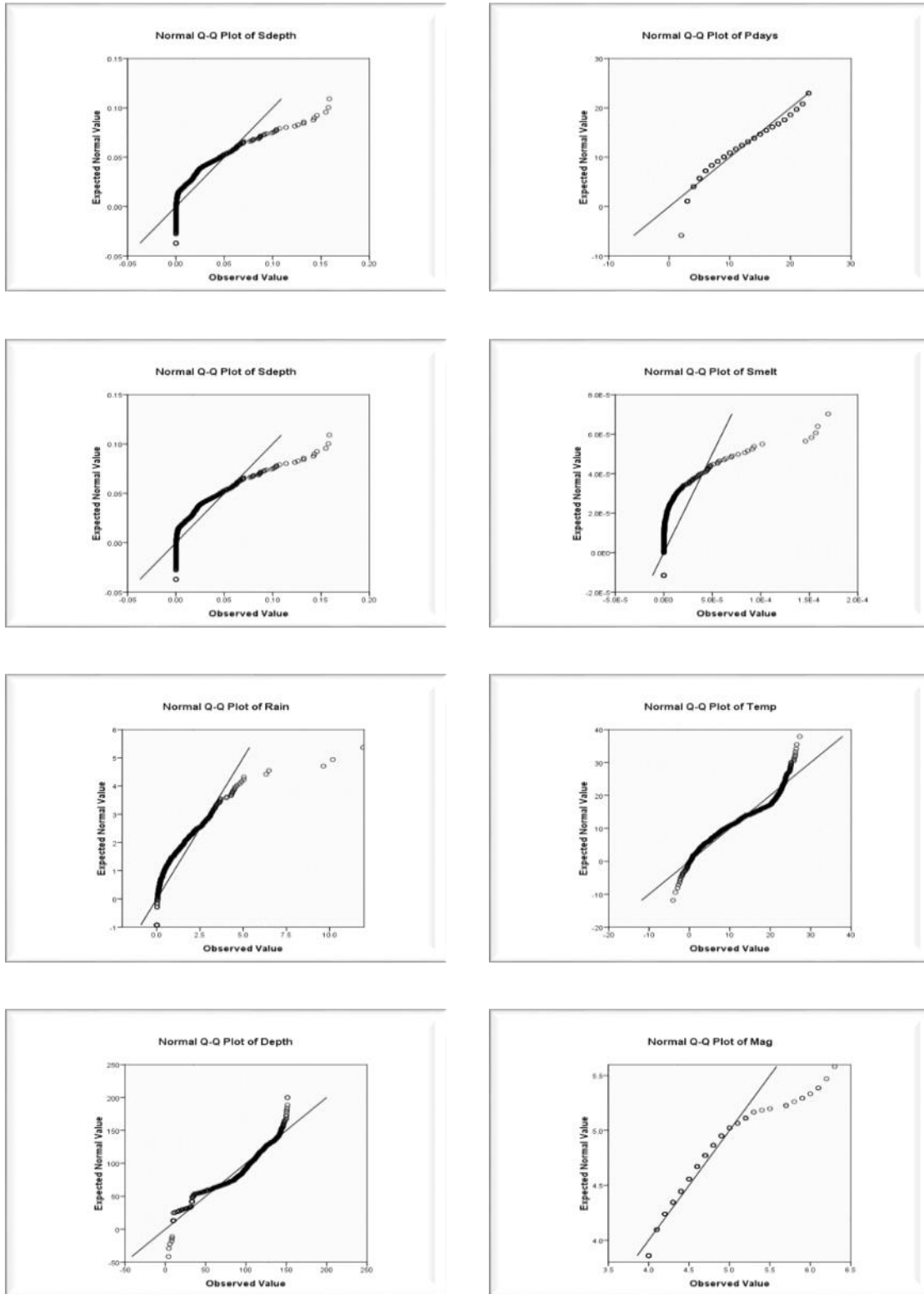


Figure 14: The q-q plot of various atmospheric variables showing near to normal line in the graph representing linear and normally distributed data for all values above threshold of our preset 2 standard deviation criteria. The data with linearity was used for further analysis. Only snow melt deviates anomalously from linearity yet it does not hinder our further analysis from giving a valid and appropriate result.

Factor Analysis

First Factor Analysis

First factor analysis was conducted with a Varimax rotation matrix (rotation cleans up the interpretation). This is based on a preset that the independent variables are in orthogonal relationship with the dependent variable, meaning there is no clear relationship between them. Hence following results were obtained (Tables 6-8 and Figure 15).

Table 6: Descriptive analysis of variables. It gives mean, standard deviation and analysis number of the variables.

	Mean	Std. Deviation	Analysis N
Mag	4.4453	.37441	523
Depth	82.9287	41.01239	523
Temp	13.0283	8.19065	523
Rain	1.0565	1.41830	523
Smelt	.0000	.00002	523
Sdepth	.0205	.02916	523
SLHF	42.1563	38.46580	523
Pdays	10.6482	5.77471	523
AccuRain	14.5264	9.39423	523
SLHFhigh	59.1377	43.36546	523

Table 7: The Kaiser-Meyer-Olkin Measure of Sampling Adequacy (KMO) and Bartlett's test of sphericity. This table displays two tests that suggest the suitability of our data for structure detection. The KMO is a statistic that indicates the proportion of variance in the variables that might be caused by underlying factors. High value (> 0.5) indicates that a factor analysis may be useful with our data. If the value were less than 0.50, the results of the factor analysis probably won't be very useful. The Bartlett's tests the hypothesis that our correlation matrix is an identity matrix, which would indicate that our variables are unrelated and therefore unsuitable for structure detection. However, small values (less than 0.05) of the significance level indicate that a factor analysis may be useful with our data.

Kaiser-Meyer-Olkin Measure of Sampling Adequacy.		.673
Bartlett's Test of Sphericity	Approx. Chi-Square	1.217E3
	df	45
	Sig.	.000

Table 8: Shows the total variance explained. The first three components have a cumulative variance of more than 53%.

Component	Initial Eigenvalues			Rotation Sums of Squared Loadings		
	Total	% of Variance	Cumulative %	Total	% of Variance	Cumulative %
1	2.714	27.142	27.142	2.654	26.537	26.537
2	1.351	13.513	40.655	1.410	14.097	40.634
3	1.252	12.523	53.178	1.254	12.544	53.178
4	.997	9.967	63.145			
5	.949	9.494	72.639			
6	.907	9.066	81.705			
7	.739	7.386	89.091			
8	.619	6.191	95.282			
9	.288	2.879	98.161			
10	.184	1.839	100.000			

Extraction Method: Principal Component Analysis.

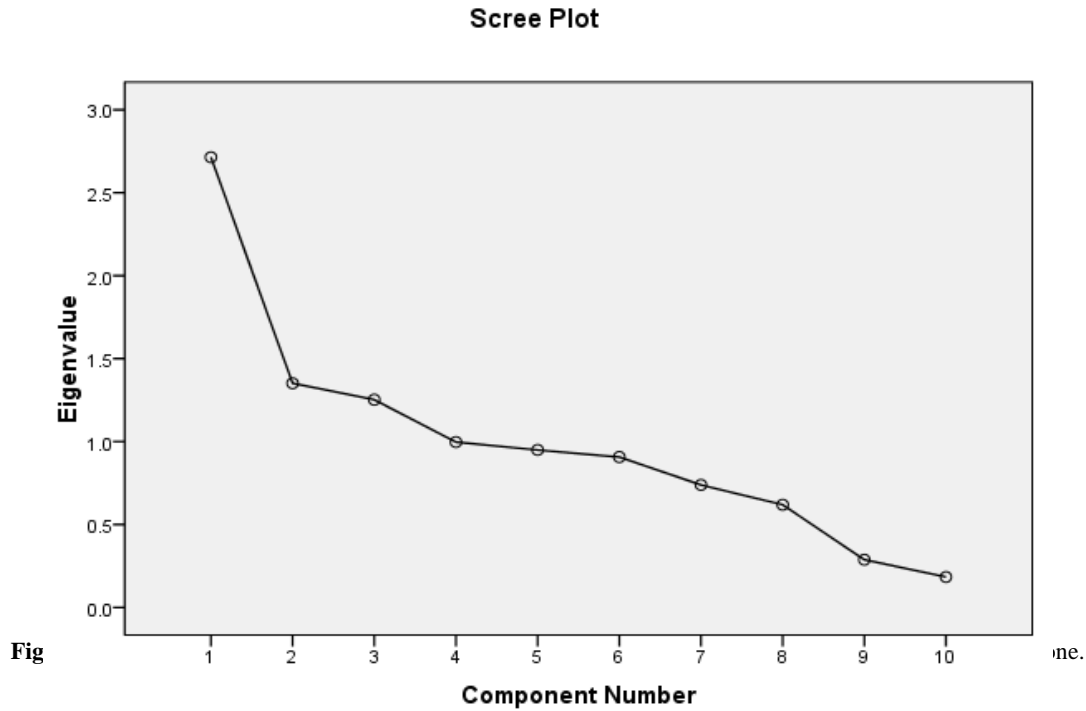


Table 9: Of Varimax rotation factor analysis, the rotated component matrix results in three leading components. The loadings with value less than 0.1 are forfeit to better understand the data.

	Component		
	1	2	3
Temp	.923		
SLHFhigh	.849	.107	.206
SLHF	.835	.271	
Sdepth	-.597	.386	.326
Smelt	.133	.723	-.103
Rain		.682	
Depth		-.376	.349
AccuRain			.727
Pdays		-.140	-.510
Mag		.156	-.414

Extraction Method: Principal Component Analysis.
 Rotation Method: Varimax with Kaiser Normalization.
 a. Rotation converged in 5 iterations.

First Multiple Regression Model

As per findings of the first factor analysis, a first regression model is constructed between magnitude as dependent variable and SLHF high, SLHF, snow depth, snow melt, rain, depth, and preceding days as independent variables (Table 9). This model has an R square value of 0.015 meaning this model explains 1.5% of variance found in the data. The adjusted R square value is 0.002, which explains 0.2% of variability in the magnitude by the independent variables.

A regression model is developed, with an R² of 0.015. The results of ANOVA show the P-value of 0.326 which indicates the model significance by 67%. However, since the predictor variables or the independent variables in this model gave a very low significance value, therefore this model was not preferred and rejected.

Second Multiple Regression Model

A second regression model is constructed between magnitude as dependent variable and SLHF high, snow depth, snow melt, depth, accumulated rain, and preceding days as dependent variables. The analysis is conducted as per the results of the Varimax rotation matrix to check the significance of predictors in predicting the dependent variable (Table 9). This model has an R square value of 0.012 meaning, this model also explains 1.2% of variance found in the data. The adjusted R square value is 0.001 which describes 0.1% variability in magnitude by the independent variables.

A significant regression equation was found ($F(6, 516) = 1.046, p < .394$). The results of ANOVA show a P-value of 0.394. This model has a 60% significance value. Moreover, almost all independent variable loadings have significant values greater than 0.3. However, this model is also not preferred due to its smaller significance values.

Second Factor Analysis

This factor analysis was conducted using Rotation matrix Oblimin, which infers that there is a direct relationship between the dependent variable and the independent variables. The Oblimin rotation is a general form for acquiring oblique rotations used to transform vectors associated with factor analysis to simple structure (Table 10-13) and Figure 16.

Table 10: Explains the descriptive statistics of all the variables, including their mean, standard deviation and number of analysis quantities.

	Mean	Std. Deviation	Analysis N
Mag	4.4453	.37441	523
Depth	82.9287	41.01239	523
Temp	13.0283	8.19065	523
Rain	1.0565	1.41830	523
Smelt	.0000	.00002	523
Sdepth	.0205	.02916	523
SLHF	42.1563	38.46580	523
Pdays	10.6482	5.77471	523
AccuRain	14.5264	9.39423	523
SLHFhigh	59.1377	43.36546	523

Table 11: Matrix showing correlation and significance of independent variables and earthquakes magnitude.

		Mag
Correlation	Mag	1.000
	Depth	-.076
	Temp	-.005
	Rain	.042
	Smelt	.031
	Sdepth	-.021
	SLHF	-.053
	Pdays	.041
	AccuRain	-.058
	SLHFhigh	-.036
Sig. (1-tailed)	Mag	

	Depth	.042
	Temp	.457
	Rain	.171
	Smelt	.237
	Sdepth	.315
	SLHF	.114
	Pdays	.177
	AccuRain	.095
	SLHFhigh	.203
a. Determinant = .095		

a. Determinant = .095

Table 12: This table shows results of the KMO and the Bartlett's test. The KMO results show a value greater than 0.6, which is a good value that indicates the dataset can be used for further analysis. The Bartlett's test show significance value lower than 0.001 which again offers a pass to proceed to further analysis.

Kaiser-Meyer-Olkin Measure of Sampling Adequacy.		.673
Bartlett's Test of Sphericity	Approx. Chi-Square	1.217E3
	df	45
	Sig.	.000

Table 13: Explains total variance found in the dataset. As the eigen values were set to be > 1, three main components were extracted that cumulatively explained more than 53% of variance in the data.

Component	Initial Eigenvalues			Rotation Sums of Squared Loadings
	Total	% of Variance	Cumulative %	Total
1	2.714	27.142	27.142	2.668
2	1.351	13.513	40.655	1.420
3	1.252	12.523	53.178	1.254
4	.997	9.967	63.145	
5	.949	9.494	72.639	
6	.907	9.066	81.705	
7	.739	7.386	89.091	
8	.619	6.191	95.282	
9	.288	2.879	98.161	
10	.184	1.839	100.000	

Extraction Method: Principal Component Analysis.

a. When components are correlated, sums of squared loadings cannot be added to obtain a total variance.

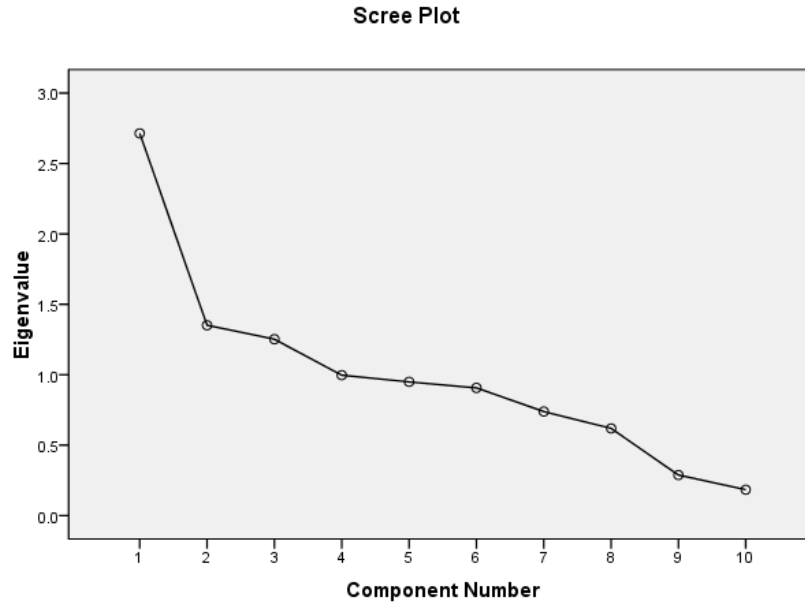


Figure 16: The scree plot graphically shows that three components are above the eigen value of one.

Table 14: Of Oblimin rotation factor analysis, the rotated component matrix results in three leading components. The loadings with value less than 0.1 are forfeit to better understand the data.

	Component		
	1	2	3
Temp	.923		
SLHFhigh	.848		.212
SLHF	.831	.249	
Sdepth	-.604	.412	.326
Smelt	.121	.717	
Rain		.682	
Depth		-.366	.347
AccuRain			.727
Pdays		-.154	-.511
Mag		.147	-.413

Extraction Method: Principal Component Analysis.
Rotation Method: Oblimin with Kaiser Normalization.

a. Rotation converged in 6 iterations.

Third Multiple Regression Analysis

The pattern matrix results convey that the third multiple regression model should be constructed between SLHF, snow depth, snow melt, rain, depth, preceding days and magnitude (Table 14). The regression analysis results show that R square is 0.011 and adjusted R Square is 0.002. By comparing these results with the results of first and second multiple regression analyses, we find that the significance of coefficient variables affecting magnitude shown are already very low - the highest significance is of approximately 60%.

Fourth Multiple Regression Analysis

As per the results of the second factor analysis, a fourth multiple linear regression model was constructed to predict magnitude of earthquake based on SLHF, snow depth, snow melt, rain, depth,

and preceding days (Tables 14-17). Preliminary analysis was performed to ensure that there is no violation of the assumption of normality, linearity and collinearity.

Table 15: Data statistics describing mean, standard deviation and number of values for the variables used in fourth multiple regression model.

	Mean	Std. Deviation
Mag	4.4453	.37441
Pdays	10.6482	5.77471
Depth	82.9287	41.01239
Rain	1.0565	1.41830
snow melt in mm	.0074	.02065
snow depth in mm	20.4943	29.15715
SLHF	42.1563	38.46580

Table 16: Correlations and significances of the loaded variables with the magnitude of earthquakes.

		Mag
Pearson Correlation	Mag	1.000
	Pdays	.041
	Depth	-.076
	Rain	.042
	Smelt	.031
	Sdepth	-.021
	SLHF	-.053
Sig. (1-tailed)	Mag	.
	Pdays	.177
	Depth	.042
	Rain	.171
	Smelt	.237
	Sdepth	.315
	SLHF	.114

Table 17: All requested variables are entered for analysis.

Model	Variables Entered	Variables Removed	Method
1	SLHF, Depth, Pdays, Rain, snow depth in mm, snow melt in mm ^a	.	Enter

a. Dependent Variable: Mag

Table 18: The table shows the summary of multiple linear regression model and overall t-statistics. The adjusted R^2 of our model is .004 with the $R^2 = .015$. This means that the linear regression explains 1.5 % of the variance in the data. The Durbin-Watson $d = 1.962$, which lies between critical values of $1.5 < d < 2.5$. Hence, it can be assumed that there is no first order linear auto-correlation in our multiple linear regression data.

Model	R	R Square	Adjusted R Square	Std. Error of the Estimate	Durbin-Watson
1	.124 ^a	.015	.004	.37367	1.962

a. Predictors: (Constant), SLHF, Depth, Pdays, Rain, snow depth in mm, snow melt in mm

b. Dependent Variable: Mag

The adjusted R square controls the overestimates of the population R square which is present from high collinearity and small variable ratios in the dataset (Table 18). The adjusted value of R square 0.004 tells us that 0.4 of variability in magnitude is explained by the independent variables. Moreover, the "Std. Error of the Estimate (SEE)" is the standard deviation of the residuals. Therefore, if the R^2 value rises then the SEE will surely decrease. In conclusion, a better fit dataset has very less estimation error. As per this analysis, our estimated magnitude by this model is susceptiblely wrong by 0.37 units.

Table 19: The ANOVA table, reports how well the regression equation fits the data (i.e., predicts the dependent variable).

Model	Sum of Squares	df	Mean Square	F	Sig.	
1	Regression	1.126	6	.188	1.345	.236 ^a
	Residual	72.050	516	.140		
	Total	73.176	522			

a. Predictors: (Constant), SLHF, Depth, Pdays, Rain, Sdepth, Smelt

b. Dependent Variable: Mag

The ANOVA table presents results of the F test and the significance value (Table 19). The primary objective of doing ANOVA is to check whether the model follows the null or the alternative hypothesis. The null hypothesis for the F test of regression is that the model has no explanatory power, which is similar as saying that all the independent variables have zero coefficient, meaning none of the independent variables help to predict the earthquakes magnitude. In other words, the model is of no use. We reject the null hypothesis by looking at the P- value that is also called significance value. The Sig. column, in the ANOVA table shows a value of 0.236 which indicates the statistical significance of the multiple regression model is more than 76%.

Table 20: The variable coefficients table gives the coefficients and significance of independent variables

Model		Unstandardized Coefficients		Standardized Coefficients	t	Sig.
		B	Std. Error	Beta		
1	(Constant)	4.498	.055		81.426	.000
	Preceding days	.003	.003	.039	.876	.381
	Depth	-.648E-4	.000	-.071	-1.611	.108
	Rain	.014	.012	.053	1.166	.244
	Snow melt	.570	.848	.031	.673	.501
	Snow depth	-.562E-4	.001	-.044	-.957	.339
	SLHF	-.793E-4	.000	-.082	-1.718	.086

a. Dependent Variable: Mag

Through Table 20 we find that participants' predicted magnitude is equal to $4.498 - 7.93E-4$ (SLHF) + $-5.62E-4$ (snow depth) + 0.57 (snow melt) + 0.014 (rain) + 0.003 (preceding days), where SLHF is measured in Watts per square meter, snow depth is measured in mm of water equivalent, snow melt is measured in mm of water equivalent, rain is measured in mm and preceding time is measured in days. As per the analyzed empirical rule, the SLHF has 91%, rainfall has 76%, Snow depth has 66% and preceding days has 61% significance with magnitude - whereas the snow melt has greater standard error and very low correlation with the magnitude. To check the linearity of residual data, a histogram and a normal p-p plot of residuals is made (Figures 17-18). The analysis justifies the linearity of the residual data.

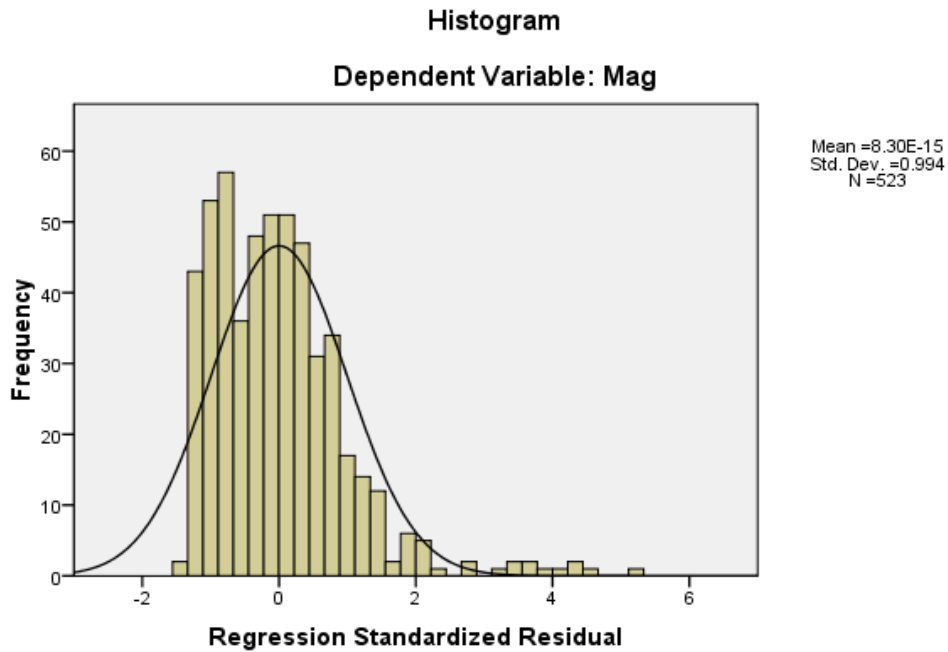


Figure 17: Histogram showing the regression of the residual data.

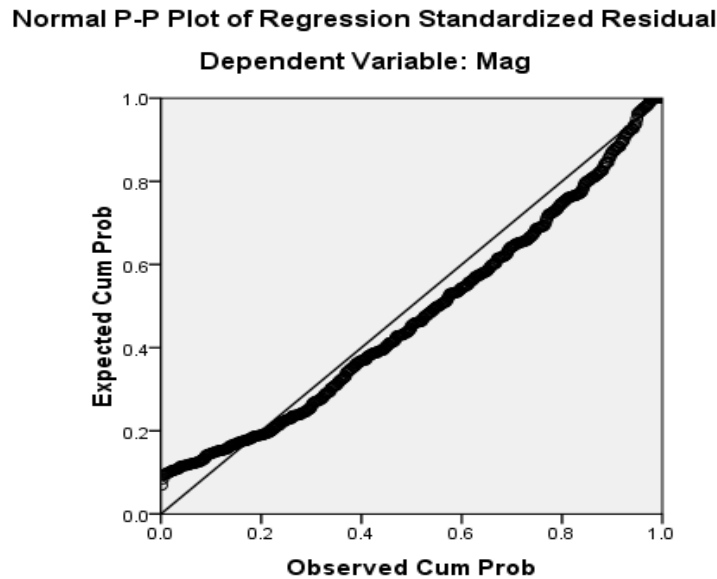


Figure 18: Normal p-p plot showing the regression of the residual data.

Owing to smaller significances the first, the second and the third multiple regression models are forfeited. Nevertheless it is seen that the fourth analyzed multiple regression model has a significance value of 76% (higher than all analyzed), and therefore is selected.

Hence, it is concluded that the fourth multiple linear regression model is the preferred empirical rule for projecting magnitude of earthquakes by using the following equation:

$$\text{Mag} = 0.014 \times (\text{Rain}) - 7.93\text{E-}4 \times (\text{SLHF}) + 0.003 \times (\text{Preceding days}) - 5.62 \times 10^{-4} \times (\text{Snow depth}) + 0.57 \times (\text{Snow melt}) + 4.498$$

Conclusion

A hypothesis based on sensitivity analysis is taken as a reason to believe that earthquake's magnitude and depth is related to rainfall, temperature, SLHF, snow melt and snow depth. Hence to verify our assumption, factor analysis is conducted for the dataset where the earthquake events had atmospheric variables as precursors. The output results in different variables loaded together with the factor they are dependent on as interpreted in component matrix.

The factor analysis had ten variables viz. magnitude, depth, temperature, rainfall, snow melt, snow depth, SLHF, preceding days, accumulated rainfall and maximum values of SLHF during the preceding times of earthquakes. Of all the various atmospheric variables, the SLHF shows the highest number of linkage with the earthquakes which is followed by rainfall, then snow depth and lastly the preceding days.

The findings of this research are beneficial as precursors of earthquake such as atmospheric anomalies showed plausible linkages via sensitivity and factor analyses. In this way, we can proclaim that in cases where no major significant precursors such as synchronous emission spectra, electric and magnetic field, the concentration of gas emissions, groundwater level changes, and ground temperature changes are observed then there is a possibility for the atmospheric variables to be the precursors of those earthquakes in the region.

References

- Daneshvar, M. R. M., M. Khosravi, T. Tavousi, 2014:** Seismic triggering of atmospheric variables prior to the major earthquakes in the Middle East within a 12-year time-period of 2002-2013. *Nat Hazards* 74:1539–1553. doi: 10.1007/s11069-014-1266-5
- Dee, D. P., Uppala, S. M., Simmons, A. J., Berrisford, P., Poli, P., Kobayashi, S., Andrae, U., Balmaseda, M. A., Balsamo, G., Bauer, P., Bechtold, P., Beljaars, A. C. M., van de Berg, L., Bidlot, J., Bormann, N., Delsol, C., Dragani, R., Fuentes, M., Geer, A. J., Haimberger, L., Healy, S. B., Hersbach, H., Hólm, E. V., Isaksen, I., Kållberg, P., Köhler, M., Matricardi, M., McNally, A. P., Monge-Sanz, B. M., Morcrette, J.-J., Park, B.-K., Peubey, C., de Rosnay, P., Tavolato, C., Thépaut, J.-N. and Vitart, F. 2011:** The ERA-Interim reanalysis: configuration and performance of the data assimilation system. *Q.J.R. Meteorol. Soc.*, 137: 553–597. doi: 10.1002/qj.828
- Freund, F.T., A. Takeuchi, B. W. S. Lau, 2006:** Electric currents streaming out of stressed igneous rocks - A step towards understanding pre-earthquake low frequency EM emissions. *Phys Chem Earth* 31:389–396. doi: 10.1016/j.pce.2006.02.027
- Kanamori, H., 2001:** Chapter 11 Energy budget of earthquakes and seismic efficiency. Academic Press
- Lachenbruch, A. H., J. H. Sass, 1992:** Heat-Flow from Cajon Pass, Fault Strength, and Tectonic Implications. *J Geophys Res Earth* 97:4995–5015. doi: 10.1029/91JB01506
- Larkina, V. I., V. V. Migulin, O. A. Molchanov, et al ,1989:** Some statistical results on very low frequency radiowave emissions in the upper ionosphere over earthquake zones. *Phys Earth Planet Inter* 57:100–109. doi: 10.1016/0031-9201(89)90219-7
- Lomnitz, C., 1996:** Book review fundamentals of earthquake prediction, *Cinna Lomnitz* ,. 20:303–304.

- Martinelli, G., 2000:** Contributions to a History of Earthquake Prediction Research. *Seismol Res Lett* 71:583–588.
- Pulinets, S. A., D. Ouzounov, A. V. Karelin et al, 2006:** The physical nature of thermal anomalies observed before strong earthquakes. *Phys Chem Earth* 31:143–153. doi: 10.1016/j.pce.2006.02.042
- Pulinets, S. A., D. P. Ouzounov, A. V. Karelin, D. V. Davidenko, 2015:** Physical bases of the generation of short-term earthquake precursors: A complex model of ionization-induced geophysical processes in the lithosphere-atmosphere-ionosphere-magnetosphere system. *Geomagn Aeron* 55:521–538. doi: 10.1134/S0016793215040131
- Pulinets, S., D. Ouzounov, 2011:** Lithosphere-Atmosphere-Ionosphere Coupling (LAIC) model - An unified concept for earthquake precursors validation. *J Asian Earth Sci* 41:371–382. doi: 10.1016/j.jseaes.2010.03.005
- Reasenber, P. A., 1999:** Foreshock occurrence before large earthquakes. *J Geophys Res* 104:4755. doi: 10.1029/1998JB900089
- Rikitake, T., 1968:** Earthquake prediction. *Earth-Science Rev* 4:245–282. doi: 10.1016/0012-8252(68)90154-2
- Svensmark, H., J. O. P. Pedersen, N. D. Marsh et al, 2007:** Experimental evidence for the role of ions in particle nucleation under atmospheric conditions. *Proc R Soc A Math Phys Eng Sci* 463:385–396. doi: 10.1098/rspa.2006.1773
- Tramutoli, V., V. Cuomo, C. Filizzola, et al, 2005:** Assessing the potential of thermal infrared satellite surveys for monitoring seismically active areas: The case of Kocaeli (??zmit) earthquake, August 17, 1999. *Remote Sens Environ* 96:409–426. doi: 10.1016/j.rse.2005.04.006
- Tronin, A. A., M. Hayakawa, O. A. Molchanov, 2002:** Thermal IR satellite data application for earthquake research in Japan and China. *J Geodyn* 33:519–534. doi: 10.1016/S0264-3707(02)00013-3
- Varotsos, P. A., N. V. Sarlis, E. S Skordas, M. S. L. Varotsos, 2017:** M W9 Tohoku earthquake in 2011 in Japan: precursors uncovered by natural time analysis. *Earthq Sci*. doi: 10.1007/s11589-017-0189-0
- Wu, L., S. Liu, 2009:** Remote Sensing Rock Mechanics and Earthquake Thermal Infrared Anomalies. In: *Jedlovec GBT-A in G and RS* (ed). InTech, Rijeka, p Ch. 34
- Yamauchi, T., 1987:** ANOMALOUS STRAIN RESPONSE TO RAINFALL IN RELATION TO EARTHQUAKE OCCURRENCE IN THE TOKAI AREA, JAPAN. *J Phys Earth* 35:19–36. doi: 10.4294/jpe1952.35.19
- Zhang, W., J. Zhao, W. Wang, et al, 2013:** A preliminary evaluation of surface latent heat flux as an earthquake precursor. *Nat Hazards Earth Syst Sci* 13:2639–2647. doi: 10.5194/nhess-13-2639-2013